Pairing correlations in two-dimensional large-size Cu-O clusters: Nonlocal world-line Monte Carlo algorithm

Vladimir A. Kashurnikov
Moscow State Engineering Physics Institute (Technical University), Kashirskoe shosse 31, 115409, Moscow, Russia
(Received 7 August 1995)

A Monte Carlo world-line algorithm for a CuO_2 plane based on a breakup of the plane into five-site cells, CuO_4 has been suggested. The algorithm has fast convergency and gives the possibility of investigating the superconducting state symmetry. The calculation of pairing correlation functions was made with an advent of additional imaginary-time slices to the Monte Carlo scheme. The characteristics of a two-dimensional Cu-O cluster with number of sites $N_a=768$ (16×16 CuO_2 cells) were calculated. It has been shown within the chosen interval of parameters of the Emery Hamiltonian ($U_d=6t$, $\varepsilon=1-3t$, $U_p=V=0$), temperatures ($T\geqslant0.125t$), and carrier concentrations ($0.7\leqslant x\leqslant1.5$) that (i) the long-range off-diagonal order associated with the superconducting state was not observed in the thermodynamic limit in any pairing channels and (ii) a tendency to divergence in s^* channels and $d_{x^2-y^2}$ channels, which is noted as the temperature decreases, is due to the antiferromagnetic ordering rather than the superconducting pairing. If the carrier concentration x is equal to 1.0 (undoped dielectric state) the pairing correlations have maximum amplitude and demonstrate clear antiferromagnetic ordering in the copper sublattice, and the characteristic correlation length is close to the earlier-reported antiferromagnetic length.

I. INTRODUCTION

Recently the discussion of the high-temperature superconductivity is concentrated basically around a problem of the superconducting order parameter's symmetry.[1,2] The solution of this question would give additional information on the nature of pairing interaction and considerably reduce the number of discussed theoretical models.[3–5]

In experimental works an unambiguous answer to the type of symmetry of the superconducting order parameter is not yet given. Indeed, the measurements of the gap's anisotropy in Josephson contacts and superconducting quantum interference devices,[6–11] as well as the experiments on the nuclear magnetic resonance,[12] Raman scattering,[13] and tunnel microscopy,[14] are interpreted as proof of $d_{x^2-y^2}$ symmetry, while the other data (for example, angular photoemission[15] and Josephson-junction measurements[16]) specify s symmetry.

It must be emphasized, that in the majority of cases[6–17] a strong anisotropy of the order parameter's modulus is observed; however, the occurrence of the zeroth superconducting order parameter does not prove d symmetry, since the order parameter can also be equal to zero at the strong anisotropic s pairing.[2,3] To check the existence of d pairing it is necessary to measure the order parameter's phase.[2] In addition, the same results have been interpreted as mixed s^* and $d_{x^2-y^2}$ pairing.[17,18]

The small correlation length scale, weak isotope effect, and a number of other abnormal properties of high-temperature superconductivity (HTSC) provided a basis for research of the high-temperature superconductivity nature within the framework of nonphonon models. In this connection the most adequate models of HTSC are those of Hubbard[19] and Emery.[20] In our opinion, the Emery model (as an extended Hubbard model) is the best one, since it immediately describes the basic structural element of high-temperature superconductors — the CuO_2 plane. The analytical study is a stubborn problem in the context of these models,[21,22] which is why the exact diagonalization[23,24] and Monte Carlo[25–27] (MC) methods are of paramount importance, because they enable us, in principle, to calculate the model characteristics without the approximation and simplifications of the model Hamiltonian as well as without recourse to the ground-state type.

The exact diagonalization method was used for the Cu_4O_8 cluster of the Emery model to study the binding energies and the correlation functions of excess carriers.[28–35] It was asserted that there is a tendency to carrier pairing in a wide range of model parameters.

As to the question of the symmetry of pairing, the calculation of pairing correlations in the Cu_4O_8 cluster by exact diagonalization for s, s^*, and $d_{x^2-y^2}$ channels was interpreted as being indicative of the prevalence of s^* symmetry.[36] The exact diagonalization data in the framework of the t-J model[37] suggest d symmetry.

Unfortunately, the major restriction of the exact diagonalization method, the small size of the system, does not allow us to reveal unequivocally the existence of superconductivity in some pairing channel, since to attain these ends one needs to prove the divergence of the pairing correlators in the momentum space in the thermodynamic limit.[1,2] Therefore, to trace the scaling of the system characteristics with respect to the cluster size, one should use quantum Monte Carlo methods,[25–27] which enable us to calculate the thermodynamic averages of physical quantities of large clusters with $N_a=100-200$. The shortcoming of these methods is the inaccessibility of the low-temperature region, where statistical fluctuations make the evaluation of quantities impossible. Nevertheless, it is believed that MC data over an achieved temperature range may be sufficient for the study of the

long-size correlation effects determining the superconducting state.[27] In particular, it has been shown that a divergence of the pairing in the s channel is observed at any electron filling for a single-band two-dimensional (2D) attractive Hubbard model.[38] On the other hand, in the case of the repulsion in the 2D Hubbard model,[39] s pairing was not observed (the correlations do not diverge as $N_a \to \infty$). The same result was reported in Ref. 40.

In the case of the Emery model, the absence of the long-range off-diagonal order in the s channel of the pairing in the thermodynamic limit has been demonstrated by the pairing correlation scaling.[27] Alternatively, there is a great body of Monte Carlo simulation data[41–46] in which a systematic analysis of the finite-size effects in pairing correlators and susceptibilities is not pursued, however, the authors come to a conclusion about the feasibility of s^* and $d_{x^2-y^2}$ channels of pairing for the single-band 2D Hubbard model with repulsion,[41] the t-J model,[17] and the Emery model.[42–45]

Thus, there is a need to perform the pairing correlation scaling for revealing the pairing in the s^* and $d_{x^2-y^2}$ channels in the thermodynamic limit for the Emery model. It must be underscored that the maximum cluster in the CuO_2 plane calculated by the currently available Monte Carlo methods is 8×8 CuO_2 cells ($N_a=192$). Moreover, the scaling data are presented only for two clusters: 4×4 and 8×8 cells.[27] The main data about the symmetry of the pairing have been derived from the calculation of the systems with 4×4 and 6×6 CuO_2 cells ($N_a=48$ and 108, respectively).[42] Notice that the real correlation length scale is close to the linear size of these clusters.[1,26]

For the standard determinant and variational MC algorithms, the time taken for convergence grows with the system size as N_a^3. This restricts the potentialities of these methods for clusters with numbers of sites $N_a > 200$.

Recently the new world-line Monte Carlo algorithm for the 2D Cu-O clusters was developed.[26] This algorithm has fast convergence (the Monte Carlo simulation time is proportional to N_a). However, the known limitation of the world-line MC — the impossibility of calculating the thermodynamic averages that do not conserve the fermion number locally (within the CuO_2 cells) — does not allow to use this algorithm for studying nonlocal pairing correlations. Besides, the scheme of Ref. 26 is anisotropic in space. It does not rule out the calculation of the local characteristics but makes the study of symmetry properties rather difficult.

In this work the new world-line quantum Monte Carlo algorithm based on a breakup of the CuO_2 plane into the five-site cells CuO_4 is offered. The scheme of the method is spatially isotropic. To study the nonlocal pairing correlations, we enter an additional temporal slice into the configuration space resulting in a breakup of the fermion trajectories. All information is retrieved from this slice. This circumstance reduces the convergence rate a little, which, however, is still proportional to N_a. It is also important that the world-line MC is realized in the canonical ensemble, and the calculation is carried out at fixed filling and projection of the full spin on the z axis, which essentially reduces the configuration space.

With this method we perform the calculations of pairing correlations in the s, s^*, and $d_{x^2-y^2}$ channels for a series of 2D clusters with $N_a=48$, 108, 192, 300, 432, 588, and 768. This set of clusters makes possible the correct analysis of pairing in various channels. We show that in our temperature range ($T\sim 0.1t$, $t\cong 1$ eV) the pairing correlators tend to the constant value rather than diverging as $N_a\to\infty$, i.e., superconducting correlations vanish in the thermodynamic limit. These results are in agreement with the data[27] for s pairing. However, the problem is not solved completely: we see an essential temperature dependence of pairing correlators predominantly, because of the antiferromagnetic ordering, and, thus, we cannot rule out the possibility of a phase transition at lower temperatures.

II. PAIRING-CORRELATION FUNCTIONS IN THE EMERY MODEL

Let us consider a 2D multiband Emery model for the CuO_2 plane,[20] taking into account hybridization of the copper $d_{x^2-y^2}$ and oxygen p_x, p_y orbitals, the distinction of atoms levels on copper and oxygen sites, and the Coulomb interaction on copper sites, oxygen atoms, and between them.

The Emery Hamiltonian in the hole representation is given by

$$H=-t\sum_{\langle ik\rangle,\sigma}(d_{i\sigma}^{\dagger}p_{k\sigma}+\text{H.c.})+\varepsilon\sum_{k\sigma}n_{k\sigma}+U_d\sum_i n_{i\uparrow}n_{i\downarrow}$$
$$+U_p\sum_k n_{k\uparrow}n_{k\downarrow}+V\sum_{\langle ik\rangle,\sigma,\sigma'}n_{k\sigma}n_{k\sigma'}. \quad (1)$$

Here $d_{k\sigma}^{\dagger}$ and $p_{k\sigma}^{\dagger}$ are the creation operators for the hole at $d_{x^2-y^2}$ and p_x, p_y states, respectively; $\langle ik\rangle$ denotes summation over the nearest neighbors; index i (k) refers to the copper (oxygen) sites, $n_{i\sigma}=d_{i\sigma}^{\dagger}d_{i\sigma}$, $n_{k\sigma}=p_{k\sigma}^{\dagger}p_{k\sigma}$; t is the matrix element for the copper-oxygen hopping; ε is the difference between energies of the hole at the oxygen and copper sites, U_d, U_p, and V are the energies of Coulomb repulsion of holes at the sites of copper, oxygen, and between them, respectively. The vacuum for the Hamiltonian (1) is the electron configuration $Cu\,3d^{10}O\,2p^6$ (valence state $Cu^{+}O^{2-}$). The dielectric (undoped) state corresponds to the configuration $Cu^{2+}O^{2-}$, where the hole number $\langle N\rangle$ is equal to the number of copper sites N_{Cu}. An increase (decrease) of $\langle N\rangle$ corresponds to the hole (electron) doping of the CuO_2 plane in high-T_c superconductors.

It is known that the relative (per one elementary CuO_2 cell) carrier concentration x, which corresponds to the maximum T_c, is $x=1.1$–1.25 for hole HTSC,[1,46] and $x=0.83$–0.88 for electron HTSC.[1,47] Below, we deal with this range of concentrations.

We define equal-time pairing correlations explicitly as functions of distance,[39,42]

$$P_{\alpha}(r)=\sum_l\langle\Delta_{\alpha}(r)\Delta_{\alpha}^{\dagger}(r+l)\rangle, \quad (2)$$

where the pair field operators are

$$\Delta_{\alpha}^{\dagger}(r)=\frac{1}{\sqrt{N_{Cu}}}\sum_{\nu}g_{\alpha}(r)C_{r\uparrow}^{\dagger}C_{r+\nu\downarrow}^{\dagger}. \quad (3)$$

The summation in (2) is over all elementary cells of the CuO_2 plane. It means that the operators $C_{r\sigma}^{\dagger}$ act on equiva-

lent sites, i.e., either on the copper atoms with the coordinates R_{Cu} or on the oxygen sites with the coordinates $R_{\mathrm{Cu}}+(1/2)ai$, $R_{\mathrm{Cu}}+(1/2)aj$ (a is the lattice period). We choose such sites to be the copper ones, in conformity with the nuclear magnetic resonance data,[48] where the pairing wave function on the copper sites is higher than on the oxygen sites. In principle, the operators $C^{\dagger}_{r\sigma}$ may be linear combinations of the creation operators at different sites in the unit cell[44] (such as the singlets of Zhang and Rice[49]).

The function $g_{\alpha}(\nu)$ depends on the pairing channel type. For s pairing $g_{\alpha}(\nu)=\delta_{\nu,0}$. In case of s^* pairing $g_{\alpha}(\nu)=1$ when $\nu=\pm ai$, $\pm aj$ and $g_{\alpha}(\nu)=0$ otherwise. In the case of $d_{x^2-y^2}$ pairing $g_{\alpha}(\nu)=1$ when $\nu=\pm ai$, $g_{\alpha}(\nu)=-1$ when $\nu=\pm aj$, and $g_{\alpha}(\nu)=0$ otherwise.

If there is a long-range off-diagonal order, the Fourier component

$$P_{\alpha}(k)=\sum_{r} P_{\alpha}(r)\exp(ikr) \tag{4}$$

at $k=(0,0)$ diverges in the thermodynamic limit.[42] It immediately follows, that $P_{\alpha}(r)$ as a function of r should become progressively slower with the distance tending to the constance and demonstrating the space ordering as the size N_a increases.

It is worthwhile introducing the quantity:[39,42]

$$\bar{P}_{\alpha}(k)=\sum_{r} \bar{P}_{\alpha}(r)\exp(ikr), \tag{5}$$

where

$$\bar{P}_{\alpha}(r)=\frac{1}{N_{\mathrm{Cu}}}\sum_{1}\sum_{\nu\nu'} g_{\alpha}(\nu)g_{\alpha}(\nu')G_{\downarrow}(l+r+\nu,l+\nu') \times G_{\uparrow}(l+r,l) \tag{6}$$

and

$$G_{\sigma}(l,l')=\langle C_{l\sigma}C^{\dagger}_{l'\sigma}\rangle,$$

which is obtained from (2) by the decomposition under Wick's theorem without the anomalous averages $\langle C^{\dagger}_{\uparrow}C^{\dagger}_{\downarrow}\rangle$ and $\langle C_{\downarrow}C_{\uparrow}\rangle$. In the thermodynamic limit expression (5) tends to the constance related to the correlation length ξ. Therefore, contribution to the pairing correlations can be neglected in the presence of the long-size off-diagonal order. We notice, however, that its effect may be essential in a finite cluster, so the value $\bar{P}_{\alpha}$ is usually subtracted from (2) to improve the analysis.[39]

The criterion of the pairing correlations existence in the α channel in a finite cluster can be formulated as follows:[39] If $P_{\alpha}>\bar{P}_{\alpha}$, there are pairing correlations in the α channel; otherwise there is no pairing in the channel.

It is pertinent to note, that a calculation with the fixed filling and projection of spin S_z keeps the contribution in pairing correlators of the anomalous averages only [except for the terms in Eq. (5)], so the antiferromagnetic correlations of the type $\langle C_{\uparrow}C^{\dagger}_{\downarrow}\rangle$ and $\langle C_{\downarrow}C^{\dagger}_{\uparrow}\rangle$ are equal to zero. The latter contribution is presented necessarily in standard variational and determinant algorithms[40–45] because of the large canonical ensemble situation.

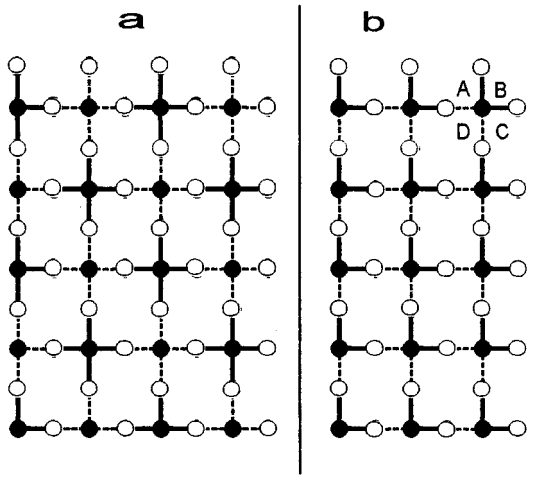

FIG. 1. Breakup of the CuO_2 plane into two types of binding [the binding of type 1 (2) is represented by solid (dashed) lines]. The label ○ stands for the oxygen atoms, the label ● marks the copper atoms: (a) is our breakup scheme and (b) is the breakup scheme of Ref. 26.

For the numerical analysis we choose the clusters having the CuO_2-plane symmetry. Thus, from all possible clusters with the square symmetry[26] we have chosen those whose basis vectors are parallel to the basis vectors of the infinite plane. An additional condition is the even number of copper sites (to provide the zeroth projection of spin S_z in the undoped state and maximum reduction of the finite-size effects). The sequence of clusters that meets our conditions is 2×2 CuO_2 cells ($N_a=12$), 4×4 CuO_2 cells ($N_a=48$), 6×6 (108), 8×8 (192), 10×10 (300), 12×12 (432), 14×14 (588), and 16×16 (768). The first cluster (Cu_4O_8) was studied earlier by exact diagonalization.[36] It has higher symmetry than the infinite CuO_2 plane and, hence, drops out from the specified set of clusters because of the strong finite-size effects.

Taking into account the correlation length data,[1,26] let us estimate the critical cluster size, which is sufficient to attain the thermodynamic limit. Because of the periodic boundary conditions, the maximum nonequivalent length $L_{\max}$ is equal to $\sim(1/2)L$ in a square cluster of the linear length L. It is reasonable to speak about the thermodynamic limit only if $L_{\max}>\xi$. Thus, the critical clusters in our sequence are those with $N_a=108$ and 192, i.e., the maximum clusters investigated by Monte Carlo methods[27,42] (the correlation length ξ is 3–4 lattice periods[1,26]).

III. NONLOCAL WORLD-LINE MONTE CARLO ALGORITHM FOR THE CuO_2 PLANE

A. Space-time breakup

We break down the Hamiltonian into two terms with different types of binds:[26]

$$H=H_1+H_2, \quad H_1=\sum_{\langle ij\rangle_1} H_{ij}, \quad H_2=\sum_{\langle ij\rangle_2} H_{ij}. \tag{7}$$

Unlike Ref. 26, we now choose the spatial breakup shown in Fig. 1(a). This breakup cuts the infinite plane into five-site

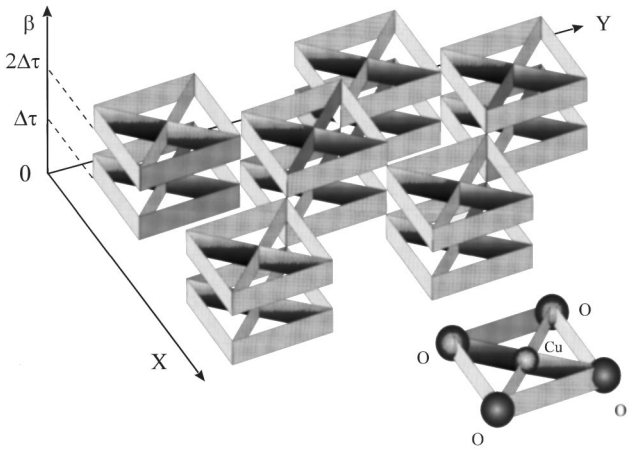

FIG. 2. (2+1)-dimensional space imaginary-time grid for the world-line MC algorithm. The fermion world lines may be switched only within the boundaries of the vertical shaded sides.

cells of CuO_4 with intercell hopping realized through the oxygen atoms. In Ref. 26 [see Fig. 1(b)] the axes *A*-*C* and *B*-*D* are nonequivalent, since the scheme forbids the carrier jumps in the diagonal direction *B*-*D* at finite temperature (diagonal hopping O-O is possible by the virtual image[26]). In our breakup scheme, these hoppings are interchangeable, so scheme (a) is spatially isotropic.

Using Trotter decomposition[50] and inserting the complete set of intermediate states for each temporal slice,[25,26] the partition function can be represented as a discrete path-integral:

$$Z=\sum_{i_1\cdots i_{2L}}\langle i_1|\exp(-\Delta\tau H_1)|i_2\rangle\langle i_2|\exp(-\Delta\tau H_2)|i_3\rangle\cdots \cdots\langle i_{2L-1}|\exp(-\Delta\tau H_1)|i_{2L}\rangle\langle i_{2L}|\exp(-\Delta\tau H_2)|i_1\rangle, \tag{8}$$

where

$$|i_m\rangle=\left|\begin{matrix} n_{1m\uparrow}n_{2m\uparrow}\cdots n_{N_a m\uparrow}\\ n_{1m\downarrow}n_{2m\downarrow}\cdots n_{N_a m\downarrow}\end{matrix}\right\rangle, \tag{9}$$

$n_{im\sigma}$ is the hole filling number of the ith lattice site with the spin σ in the mth imaginary time slice from the interval $[0,\beta]$: $\Delta\tau=\beta/L$. As the error of decomposition (8) has the order of $\Delta\tau^2 tA[A=\max(\varepsilon,\ U_d,\ U_p,\ V)$ (Refs. 25 and 26)], we typically fix $\Delta\tau\sqrt{tA}\leqslant 0.1$ for the required accuracy.

Expression (8) leads to a graphical representation. We set $2L$ as identical two-dimensional Cu-O clusters with a number of atoms N_a located one over another along the imaginary-time axis (Fig. 2). The summation in (8) is over all possible closed noncrossing trajectories. The trajectory switching takes place only within the vertical shaded sides. Each site of the (2+1)-dimensional lattice is characterized by two filling numbers $n_{m\uparrow}$ and $n_{m\downarrow}$, equal either to 0 or 1, so that there occur two different types of the trajectories ("world lines") corresponding to different spin projections. The switch from one temporal slice to the next one is defined by matrix elements of the evolution operator

$$U_{nn+1}=\langle i_n|\exp(-\Delta\tau H_{1,2})|i_{n+1}\rangle. \tag{10}$$

The total number of states in the CuO_4 cell is equal to 1024, and the evolution operator (10) is a matrix 1024×1024. To calculate the evolution operator one actually needs to perform the numerical summation:

$$U_{nn+1}=\sum_{k=0}^{\infty}\frac{1}{k!}(-\Delta\tau)^k\langle i_n|H_{1,2}|i_{n+1}\rangle^k, \tag{11}$$

cutting off the sum (11) when the required accuracy is achieved (typically, at $k\sim 20$).

In this connection we note the following two circumstances: (1) There are nonzero probabilities of the trajectory switch along the diagonal "O-O," such as virtual hopping O-O through the copper site as well as combined hoppings of the types $C^{\dagger}_{5\uparrow}C_{1\uparrow}C^{\dagger}_{5\downarrow}C_{2\downarrow}$, $C^{\dagger}_{5\uparrow}C_{1\uparrow}C^{\dagger}_{4\uparrow}C_{2\uparrow}$, etc., already in the second order on $\Delta\tau$. Hence, one should include these hole movements into Monte Carlo simulation. (2) It is necessary to know not only the absolute value of matrix element U_{nn+1} but also its sign in a given Monte Carlo configuration. The straightforward multiplication of matrices in Eq. (11) expanded in the five-site basis does not contain information about this sign, since the site numbering of an isolated cell does not coincide with the numbering of CuO_2 cells in the whole system. We proceed as follows.

First, we have calculated *exactly* an operator $\exp(-\Delta\tau H)$, i.e., obtained the sum (11) in *an analytical operator form*. This problem is a stubborn one because the number of irreducible terms (ordered with respect to the site numbering within a cell) for the Emery Hamiltonian (1) and the five-site cell CuO_4 of the type

$$C^{\dagger}_{i_2\uparrow}C_{i_2\uparrow}C^{\dagger}_{j_1\uparrow}C_{k_1\uparrow}C^{\dagger}_{j_2\uparrow}C_{k_2\uparrow}C^{\dagger}_{l_1\downarrow}C_{l_1\downarrow}C^{\dagger}_{m_1\downarrow}C_{n_1\downarrow},$$

$$C^{\dagger}_{i_1\uparrow}C_{i_1\uparrow}C^{\dagger}_{l_1\downarrow}C_{l_1\downarrow}C^{\dagger}_{m_1\downarrow}C_{n_1\downarrow},$$

etc., where

$$i,j,k,\ldots=1-5$$

(and where $i_1>i_2>i_3\cdots$, $j_1>j_2>j_3\cdots$, and $k_1>k_2>k_3\cdots$ with all indices $i,j,k,\ldots$ different) increases up to the maximum value of 63 504 because of the large number of multiplications (~ 10). Nevertheless, this problem may be solved using a computer.

Second, we have acted using the obtained operator on the wave function and got ten U_{nn+1}, including the information about its sign. The algorithm of summation over the trajectories is a standard one:[25,26] a switch of configurations by Metropolis algorithm[51] with determination of the relation of matrix element products before and after switching.

There is some peculiarity of the trajectory switching associated with the expansion of Monte Carlo cell: After switching a trajectory from an oxygen atom to the neighboring copper atom, the fermion world line can be thrown into the unshaded area of the configuration space. In this case we allow the world line to bend to escape the unshaded area. The possibility of the matrix elements signs changing, located far from the switch area but linked by the initial site numbering, should be also taken into account.

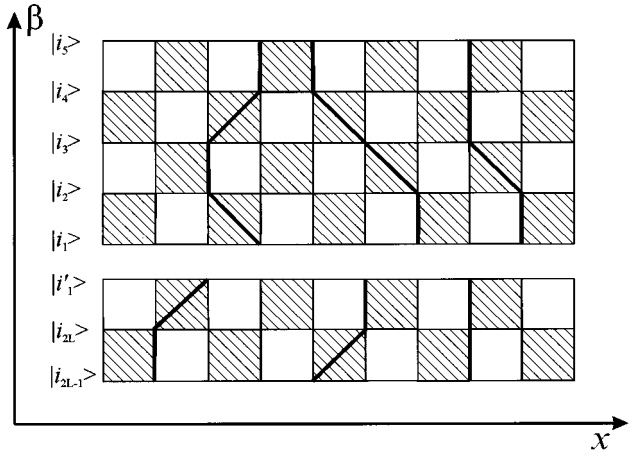

FIG. 3. The projection of the spatiotemporal grid on the vertical plane, parallel to the x axis (45° up to the a axis of the CuO_2 plane). The temporal slice for the calculation of nonlocal pairing correlators is shown. The world lines experience a breakup between states $|i\rangle$ and $|i'\rangle$.

B. Calculation of the thermodynamic averages of nonlocal physical quantities

The computation of the operators' averages that conserve fermion number locally (inside the CuO_4 cell) is done essentially in the same manner as the Monte Carlo simulation by the standard world-line algorithm.[25] So we need not dwell on the detailed description of this calculation (see, e.g., Refs. 25 and 26).

Unfortunately, the pairing correlation functions are essentially nonlocal characteristics, whose operators break off the fermion world lines and do not conserve a fermion number locally inside the CuO_4 cell. In this case, following,[25] we introduce an additional temporal slice (Fig. 3) with the possibility of the trajectories breakup. Note that the projection of a 3D classical lattice on the x-τ plane (Fig. 3) forms the standard checkerboard picture used in the 1D Monte Carlo world-line algorithm.[25] Then for the thermodynamic average of the nonlocal operator Q we have

$$\langle Q\rangle=\frac{\langle Q_1\rangle}{\langle W_1\rangle}, \tag{12}$$

$$\langle Q_1\rangle=\mathrm{tr}[\langle i_1|Q|i_{1'}\rangle U_{1',2}(k)U_{2,3}(k)\cdots U_{2L,1}(k)], \tag{13}$$

$$\langle W_1\rangle=\mathrm{tr}[\langle i_1|i_{1'}\rangle U_{1',2}(k)U_{2,3}(k)\cdots U_{2L,1}(k)]. \tag{14}$$

For computation of (12) it is necessary to realize independent Monte Carlo procedures for both the numerator and denominator in order to calculate the individual thermodynamic averages (13) and (14). We combine these processes by adding the contribution to the numerator or/and to the denominator during Monte Carlo simulation according to what matrix element ($\langle i|Q|i'\rangle$ or $\langle i|i'\rangle$) is not equal to zero. For reduction of the statistic we also exclude all MC realization where both matrix elements are equal to zero. Then all useful information is retrieved from only one time slice $\langle i|i'\rangle$. This reduces the convergence rate by a factor of $2L$, however, the rate remains proportional to the cluster size to the first power.

We notice, that for computing the temporal average of, for example, the Green's function

$$G_\sigma(i,j,\tau)=\langle C_{i,\sigma}(\tau)C^\dagger_{j\sigma}(0)\rangle, \tag{15}$$

it is necessary to insert two additional slices into the Monte Carlo scheme, one at the imaginary time 0, and one at the time τ. This average is also available within our scheme.

To attain the relevant accuracy we carry out about 10^3 Monte Carlo steps for thermalization and about 5×10^3 MC steps for calculating of averages. The statistical errors were evaluated through the correct procedure[26] and did not usually exceed a few percent in relative units.

The problem of the sign (minus sign problem) in a given algorithm does not essentially affect the convergence, since the sign of the statistical weight tends to the constant value as $T\to0$.[26] Testing the algorithm with the results of the exact diagonalization of the 12-site cluster Cu_4O_8,[36] as well as with those ones obtained by the determinant and variation MC method,[27,42] we arrive to the following conclusions.

(1) The cluster Cu_4O_8 is extremely small for a MC algorithm, which needs a sufficiently large number of degrees of freedom. Its calculation requires as much computer time as does a cluster with $N_a=300$. Nevertheless, our results are in a reasonable agreement with the exact ones. Indeed, at the hole doping ($\langle N\rangle=5$) and $U_d=6$, $\varepsilon=1$, and $T=0.125$, we have $P_d-\bar{P}_d=0.02$, $P_{s*}-\bar{P}_{s*}=0.03$, while the data of the exact diagonalization at $T=0$ (Ref. 24) give $P_d-\bar{P}_d=0.05$, $P_{s*}-\bar{P}_{s*}=0.1$, i.e., as expected, the temperature reduces the pairing correlations, and the amplitude ratio of $s*$ and d channels does not vary dramatically.

(2) The results practically coincide within the limits of the error with the data of standard MC algorithms[27,42] for clusters with $N_a=48,108,192$ using some recalculation. The point is that the pairing correlators of the type $\langle\Delta^\dagger\Delta\rangle$ are frequently calculated as opposed to Eq. (2). Nevertheless, it can be shown that this does not change the value of $P_\alpha-\bar{P}_\alpha$, and in the presence of the long-size off-diagonal order the quantity $P_\alpha-\bar{P}_\alpha$ is defined basically by the value of P_α, so that the values of $\langle\Delta^\dagger\Delta\rangle$ and $\langle\Delta\Delta^\dagger\rangle$ coincide with each other in the limit of $N_a\to\infty$.

IV. CALCULATION OF PAIRING CORRELATION FUNCTIONS

We perform the computation of pairing correlations in Cu-O clusters in the Emery model for the following parameters of the Hamiltonian (1): $\varepsilon=1-3$, $U_d=6$, and $U_p=V=0$ (in units of t). This choice is motivated by the facts that first, these parameters are suggested by experiments,[52,53] and second, only in this parameter range were the basic results on the binding energy of carriers and pairing correlations by exact diagonalization in the cluster Cu_4O_8 (Refs. 28–36) as well as on the symmetry of pairing in clusters with $N_a=48$, 108, and 192 (Refs. 42–45) by Monte Carlo method reported.

At first, we study the dependence of $P_\alpha\equiv P_\alpha(k)$ at $k=(0,0)$ on the cluster size for $\alpha=s$, $s*$, and $d_{x^2-y^2}$. In Fig. 4 we present the world-line MC data for the value of $\chi_\alpha=\sqrt{P_\alpha/N_{\mathrm{Cu}}}$ as a function of $1/\sqrt{N_{\mathrm{Cu}}}$ at the hole doping $x=1.125$ and 1.25 for clusters with $N_a=48,\ \ldots,\ 768$. It is

seen that P_α does not diverge with the increasing of N_a and tends to a constant value for all pairing channels. This result coincides with the data for s pairing for the clusters with $N_a \leqslant 192$,[27] and testifies to the absence of the long-size off-diagonal order in the thermodynamic limit (at finite temperature).

This conclusion is also supported by some of the other data of our calculation.

In Fig. 5 we present the dependence of $P_\alpha(r)$ at $\alpha = s$, s^*, and $d_{x^2-y^2}$ on the distance in units of the coordination sphere radius on the copper sublattice, which indicates that the large-size ordering is absent in the Cu-O clusters at least in this range of the Emery parameters at given temperatures. Actually, the value of $P_\alpha(r)$ will decay to zero at distances larger than the second through the third coordination sphere radius (of order of two lattice periods) for all sizes of clusters considered here. A similar spatial dependence of P_α is observed for the two-dimensional Hubbard model[38] for $\alpha = s$. Note that the cluster with $N_a = 300$ suffices to attain the thermodynamic limit, as we assumed previously from the estimation of the correlation length, so that the characteristics of larger clusters (with $N_a = 432$, 588, and 768) practically do not differ within the limits of errors from those ones for noted cluster.

Because of the rather high temperature of the calculation, the question of existence (or absence) of pairing correlations at $T \to 0$ still remains unsolved. In this connection it is reasonable to consider the temperature dependence of $P_\alpha - \bar{P}_\alpha$, whose increase with decreasing temperature in a finite cluster would demonstrate the strengthening of the correlations as the point of the phase transition is approached, if any exists (here, we subtract $\bar{P}_\alpha$ to eliminate the finite-size effects and antiferromagnetic ordering for a finite cluster). We see only this type of behavior in Fig. 6, where the temperature dependence of $P_\alpha - \bar{P}_\alpha$ for the cluster with $N_a = 300$ is plotted at the doping $x = 1.125$. Moreover, the $d_{x^2-y^2}$ channel of pairings is most sensitive to temperature.

As a check on the tendency to form large-size off-diagonal order, in Fig. 7 the dependence of $P_\alpha(r) - \bar{P}_\alpha(r)$ on r at $\alpha = s^*$ and $d_{x^2-y^2}$ is plotted at various temperatures. As temperature decreases, pronounced antiferromagnetic correlations appear with practically temperature-independent correlation length. Increasing antiferromagnetic (AF) correlations in pairing interactions is clearly seen in the temperature dependence of $P_\alpha \equiv P_\alpha(k)$ at $k = (\pi, \pi)$ (Fig. 8), since the AF contribution is the maximum in the correlator $\langle \Delta \Delta^\dagger \rangle$ for the momentum (π, π). The strong growth of correlators (for the s^* channel the increase is ~ 5 times in the interval of temperatures from $T = 0.25$ to 0.125) indicates that the main contribution to the pairing correlations is because of the antiferromagnetic ordering.[54] Besides, it is interesting to note that the characteristic length of the correlations is about six coordination sphere radii (i.e., three periods of the lattice). This value is consistent with the characteristic correlation length of the antiferromagnetic ordering obtained earlier.[26]

Thus, the temperature divergence in the s^* and $d_{x^2-y^2}$ channels of pairing is determined by antiferromagnetic correlations, and the tendency to superconducting correlations in the system is not at hand yet. Actually, we are just close to the antiferromagnetic phase transition ($T \sim 1000$ K $\sim 0.1t$),

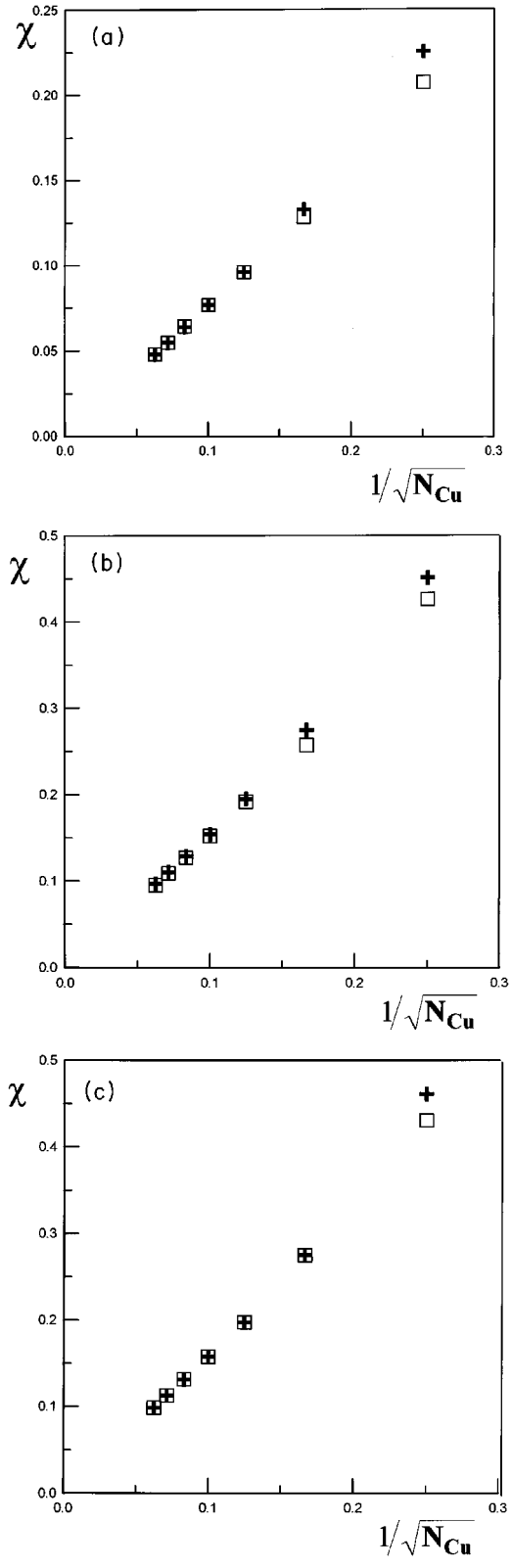

FIG. 4. $\chi_\alpha = \sqrt{P_\alpha / N_{\mathrm{Cu}}}$ as a function of $1/\sqrt{N_{\mathrm{Cu}}}$ for clusters with $N_a = 48, 108, \ldots, 768$ at the doping $x = 1.125$ (+) and $x = 1.25$ (□). $\varepsilon = 1$, $U_d = 6$, $\beta = 8$: (a) $\alpha = s$, (b) $\alpha = s^*$, and (c) $\alpha = d_{x^2-y^2}$. For Hamiltonian parameters $\varepsilon = 3$ and $U_d = 6$ and doping $x = 1.25$ the results practically coincide with the case $\varepsilon = 1$, $U_d = 6$, and $x = 1.125$ (+) for all channels of pairing.

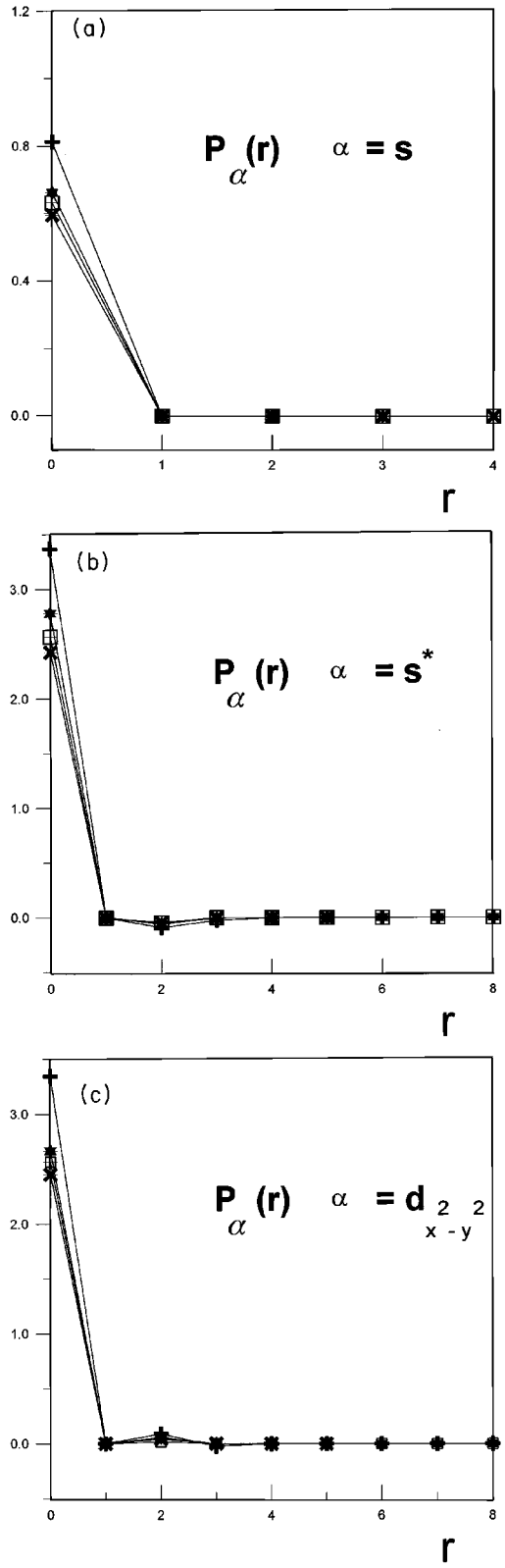

FIG. 5. Correlator $P_\alpha(r)$ as a function of the distance in units of the coordination sphere radius in the copper sublattice. Here $x=1.125$ and $N_a=48$ (+), 108 (*), 192 (□), 300 (×): (a) $\alpha=s$, (b) $\alpha=s^*$, and (c) $\alpha=d_{x^2-y^2}$. $\varepsilon=1$ and $U_d=6$, $\beta=8$. For clusters with $N_a=432$, 588, and 768 the spatial distributions practically coincide (within the error limits) with the data for $N_a=300$.

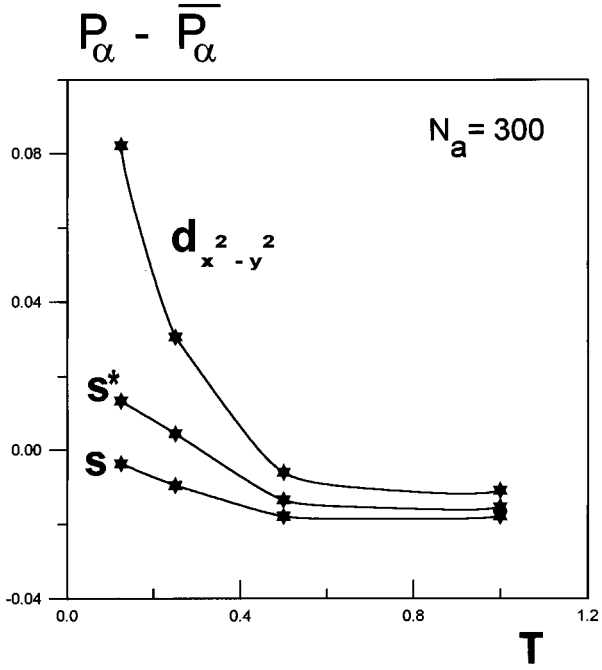

FIG. 6. The temperature dependence of $P_\alpha-\bar{P}_\alpha$ for the doping $x=1.125$ and the cluster with $N_a=300$ in s, s^*, and $d_{x^2-y^2}$ pairing channels: $\varepsilon=1$, $U_d=6$.

so that it is natural to observe the antiferromagnetic fluctuations.

Finally, we notice, that we have also carried out the computation of pairing at carrier fillings $0.7\leqslant x\leqslant 1.5$, i.e., also covering an electron doping range. Practically, the results do not differ from those above, i.e., the superconductivity is absent for all channels of pairing, as the value P_α tends to the constance with the growth of the cluster size, and the decay of spatial distribution $P_\alpha(r)$ occurs at 2–3 lattice periods [see, e.g., the data for the maximum cluster with $N_a=768$ (Fig. 9)]. The concentration dependence of $P_\alpha-\bar{P}_\alpha$ has a maximum at filling $x=1.0$, and the range of positive values corresponds to $x=0.8$–1.0 for the electron doping and $x=1.0$–1.5 for the case of the hole doping. These data are close to the results of the pairing susceptibilities' calculation;[42] however, in Ref. 42 a minimum was observed at filling $x=1.0$. Notice, that at the close concentration the antiferromagnetic ordering will be realized,[1] and the most strong antiferromagnetism should be observed only at the undoped ($x=1.0$) conditions. This fact confirms our conclusions about the antiferromagnetic ordering of hole carriers on the copper sublattice as the basic contribution to pairing correlations and about the absence of the large-size off-diagonal order.

V. CONCLUSION

A nonlocal world-line two-dimensional algorithm of the quantum Monte Carlo based on the breakup of the plane CuO_4 into the five-site cells CuO_4 is presented. Unlike the scheme reported in Ref. 26, our algorithm is spatially isotropic and thus is especially convenient for the study of the symmetry of superconducting pairing, if any kind exists. The

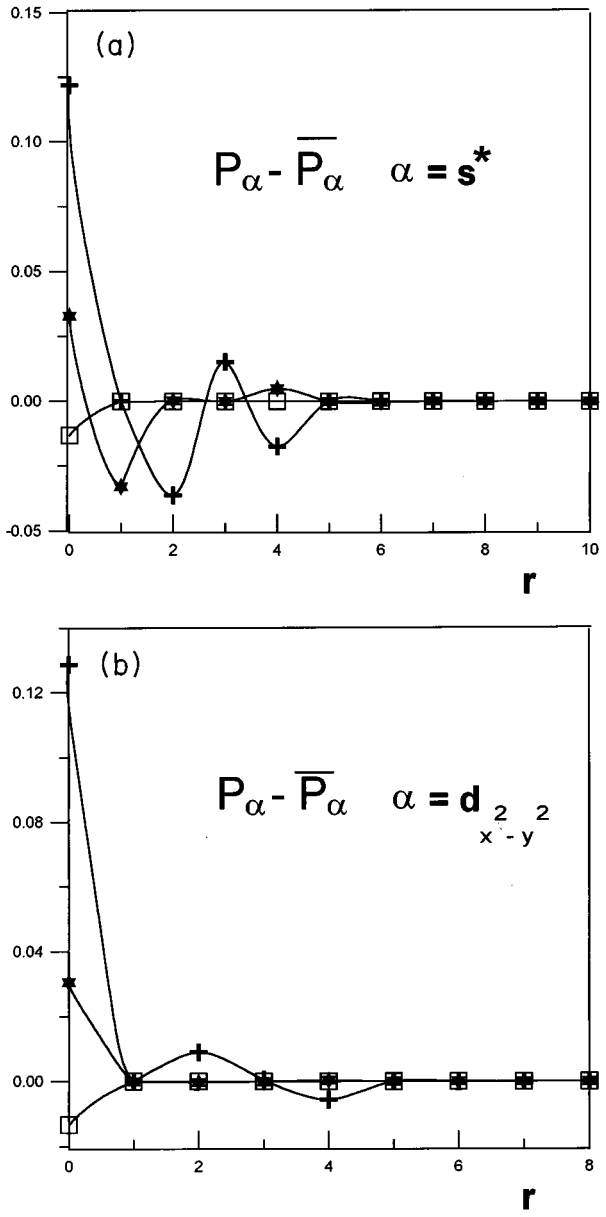

FIG. 7. The spatial distribution $P_\alpha(r)-\bar{P}_\alpha(r)$ for $N_a=300$: (a) $\alpha=s^*$ and (b) $\alpha=d_{x^2-y^2}$, $T=0.125$ (+), 0.25 (∗), and 0.5 (□); and $\varepsilon=1$, $U_d=6$, and $x=1.125$.

calculation of pairing correlation functions was carried out by inserting an additional temporal slice into Monte Carlo scheme.

The convergence rate of the algorithm is proportional to N_a (in contrast to the N_a^3 of usual methods). This gives the possibility of calculating the characteristics of Cu-O clusters up to $N_a=768$ (16×16 CuO_2 cells).

Calculation of the pairing correlation functions in the s, s^*, and $d_{x^2-y^2}$ channels of pairing leads to the following conclusions: namely, in the chosen interval of the Emery Hamiltonian parameters ($U_d=6t$, $\varepsilon=1-3t$, $U_p=V=0$), the temperature interval ($T\geqslant0.125t$), and the concentration of carriers ($0.7\leqslant x\leqslant1.5$), (a) the large-size off-diagonal order is not observed in any channel of pairing in the thermodynamic limit and (b) a tendency to divergence in s^* and

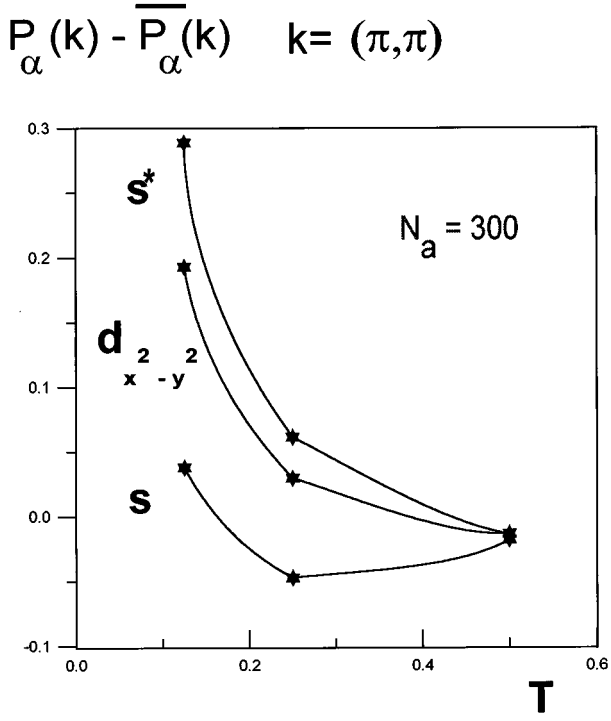

FIG. 8. The dependence of $P_\alpha(k)-\bar{P}_\alpha(k)$ at $k=(\pi,\pi)$ on the temperature in the cluster with $N_a=300$ in the s, s^*, and $d_{x^2-y^2}$ channels of pairing: $\varepsilon=1$, $U_d=6$, and $x=1.125$.

$d_{x^2-y^2}$ channels is observed as the temperature decreases, but the analysis shows the antiferromagnetic ordering as the main cause of this effect. In particular, the characteristic correlation length is close to the characteristic antiferromagnetic length.

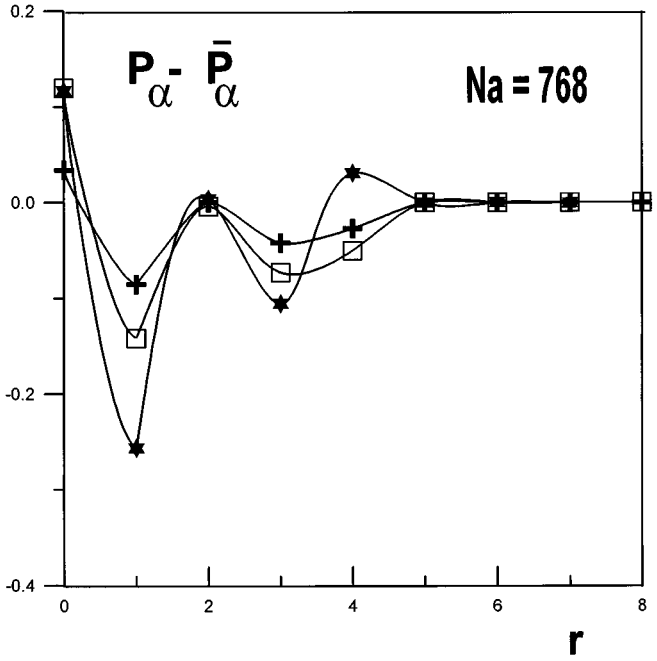

FIG. 9. The spatial distribution $P_\alpha(r)-\bar{P}_\alpha(r)$ for $N_a=768$: $\alpha=s$ (+), $\alpha=s^*$ (∗), and $\alpha=d_{x^2-y^2}$ (□); $\varepsilon=1$, $U_d=6$, and $x=1.25$.

We emphasize, that the final answer on the pairing and the symmetry is not arrived at completely: We see an essential temperature dependence of the pairing correlator because of the antiferromagnetic ordering and, thus, cannot rule out the possibility of phase transition at lower temperatures.

Basically, another criterion of the superconducting state's identification, independent from the wave-function symmetry, is possible. For example, the gauge phase can be inserted into the system,[55] and the superfluid density can be defined by the behavior of the ground-state energy as a function of the gauge phase. In particular, in the Emery model a superfluid component is not found even at the lowest (for the heat-bath Monte Carlo algorithm) temperature $T=(1/16)t$.[55]

ACKNOWLEDGMENTS

The author is grateful to V. F. Elesin, L. A. Openov, and E. G. Kholmovskii for useful discussions. The author is especially indebted to A. V. Krasheninnikov for assistance in the preparation of the graphic material, B. V. Svistunov for valuable discussions and critical reading of the manuscript, and D. V. Melnikov for critical reading of the manuscript. The research described in this publication was made possible in part by Grant No. M67300 from the International Science Foundation and Russian Government, and by Project No. 94031 from the Russian State Program ''High-Temperature Superconductivity.''

[1] E. Dagotto, Rev. Mod. Phys. **66**, 763 (1994); D. J. Scalapino, Phys. Rep. **250**, 329 (1995).
[2] V. J. Emery, Nature (London) **370**, 598 (1994).
[3] P. Mountoux and D. Pines, Nuovo Cimento D **15**, 181 (1993).
[4] S. Chakraverty, A. Sudbo, P. W. Anderson, and S. Strong, Science **261**, 337 (1993).
[5] J. R. Schrieffer, X. G. Wen, and S. C. Zhang, Phys. Rev. B **39**, 11 663 (1989).
[6] J. R. Kirtley *et al.*, Nature **373**, 225 (1995).
[7] I. Igushi and Z. Wen, Phys. Rev. B **49**, 12 388 (1994).
[8] A. G. Sun, D. A. Gajewski, M. B. Maple, and R. C. Dynes, Phys. Rev. Lett. **72**, 2267 (1994).
[9] C. C. Tsuei *et al.*, Phys. Rev. Lett. **37**, 593 (1994).
[10] D. A. Wollman *et al.*, Phys. Rev. Lett. **71**, 2134 (1993).
[11] J. Buan *et al.*, Phys. Rev. Lett. **72**, 2632 (1994).
[12] M. Bankay, M. Mali, J. Roos, and D. Brinkmann, Phys. Rev. B **50**, 6416 (1994).
[13] T. P. Devereaux *et al.*, Phys. Rev. Lett. **72**, 396 (1994); X. K. Chen *et al.*, *ibid.* **73**, 3290 (1994).
[14] J. Kane, Q. Chen, K.-W. Ng, and H.-J. Tao, Phys. Rev. Lett. **72**, 128 (1994).
[15] Hond Ding *et al.*, Phys. Rev. B **50**, 1333 (1994).
[16] P. Chaudhari and Shawn-Yu Lin, Phys. Rev. Lett. **72**, 1084 (1994).
[17] Q. P. Li, B. E. C. Koltenbah, and R. Joynt, Phys. Rev. B **48**, 437 (1993); J. E. Sonier *et al.*, Phys. Rev. Lett. **72**, 744 (1994).
[18] R. J. Kelley, J. Ma, G. Margaritondo, and M. Onellion, Phys. Rev. Lett. **71**, 4051 (1993).
[19] D. C. Mattis, Mod. Phys. Lett. B **4**, 1171 (1990); F. C. Zhang and T. M. Rice, Phys. Rev. B **37**, 3759 (1988).
[20] V. J. Emery, Phys. Rev. Lett. **58**, 2794 (1987).
[21] P. B. Littlewood, C. M. Varma, S. Scmidt-Rink, and E. Abrahams, Phys. Rev. B **39**, 12 371 (1989).
[22] S. Nimkar, D. D. Sarma, H. R. Krishnamurthy, and S. Ramasesha, Phys. Rev. B **48**, 7355 (1993).
[23] J. E. Hirsch, S. Tang, E. Loh, Jr., and D. J. Scalapino, Phys. Rev. Lett. **60**, 1668 (1988).
[24] V. F. Elesin, V. A. Kashurnikov, L. A. Openov, and A. I. Podlivaev, Zh. Éksp. Teor. Fiz. **99**, 237 (1991) [Sov. Phys. JETP **72**, 133 (1991)].
[25] J. E. Hirsch, R. L. Sugar, D. J. Scalapino, and R. Blankenbecler, Phys. Rev. B **26**, 5033 (1982).
[26] V. F. Elesin and V. A. Kashurnikov, Zh. Éksp. Teor. Fiz. **106**, 1773 (1994) [JETP **79**, 961 (1994)].
[27] M. Frick *et al.*, Phys. Rev. B **42**, 2665 (1990).
[28] L. Tan, Q. Li, and J. Callaway, Phys. Rev. B **44**, 341 (1991).
[29] J. E. Hirsch, E. Loh, Jr., D. J. Scalapino, and S. Tang, Phys. Rev. B **39**, 243 (1989).
[30] V. F. Elesin, V. A. Kashurnikov, L. A. Openov, and A. I. Podlivaev, Zh. Éksp. Teor. Fiz. **101**, 682 (1992) [Sov. Phys. JETP **74**, 363 (1992)].
[31] V. F. Elesin, V. A. Kashurnikov, L. A. Openov, and A. I. Podlivaev, Physica C **195**, 171 (1992).
[32] V. F. Elesin, V. A. Kashurnikov, and A. I. Podlivaev, Zh. Éksp. Teor. Fiz. **104**, 3835 (1993) [Sov. Phys. JETP **77**, 841 (1993)].
[33] V. F. Elesin, V. A. Kashurnikov, A. V. Krasheninnikov, and A. I. Podlivaev, Physica C **222**, 127 (1994).
[34] V. F. Elesin, V. A. Kashurnikov, A. V. Krasheninnikov, and A. I. Podlivaev, Zh. Éksp. Teor. Fiz. **105**, 1759 (1994) [JETP **78**, 951 (1994)].
[35] V. F. Elesin, V. A. Kashurnikov, L. A. Openov, and A. I. Podlivaev, Solid State Commun. **89**, 27 (1994).
[36] V. F. Elesin, A. V. Krasheninnikov, and L. A. Openov, Zh. Éksp. Teor. Fiz. **106**, 1459 (1994) [JETP **79**, 789 (1994)].
[37] D. Poilblanc, Phys. Rev. B **48**, 3368 (1993); E. Dagotto and J. Riera, *ibid.* **46**, 12 084 (1992).
[38] A. Moreo and D. J. Scalapino, Phys. Rev. Lett. **66**, 946 (1991).
[39] A. Moreo, Phys. Rev. B **45**, 5059 (1993).
[40] R. T. Scalettar, J. W. Cannon, D. J. Scalapino, and R. L. Sugar, Phys. Rev. B **50**, 13 419 (1994).
[41] R. E. Hetzel, W. von der Linden, and W. Hanke, Phys. Rev. B **50**, 4159 (1994).
[42] R. T. Scalettar, D. J. Scalapino, R. L. Sugar, and S. R. White, Phys. Rev. B **44**, 770 (1991).
[43] M. Imada, J. Phys. Soc. Jpn. **56**, 3793 (1987); **57**, 3128 (1988).
[44] G. Dopf, A. Muramatsu, and W. Hanke, Phys. Rev. B **41**, 9264 (1990).
[45] A. Bhattacharya and C. S. Wang, Phys. Rev. B **48**, 13 949 (1993).
[46] H. Zang and H. Sato, Phys. Rev. Lett. **70**, 1697 (1993).
[47] O. G. Singh *et al.*, Physica C **219**, 156 (1994).
[48] P. C. Hammel *et al.*, Phys. Rev. Lett. **63**, 1992 (1989).
[49] F. C. Zhang and T. M. Rice, Phys. Rev. B **37**, 3759 (1988).
[50] M. Suzuki, Phys. Lett. A **113**, 299 (1985).
[51] N. Metropolis *et al.*, J. Chem. Phys. **21**, 1087 (1953).

[52] A. K. McMahan, J. F. Annett, and R. M. Martin, Phys. Rev. B **42**, 6268 (1990).

[53] H. Rushan, C. K. Chew, K. K. Phua, and Z. Z. Gan, J. Phys. Cond. Matter **3**, 8059 (1991).

[54] We remind the reader that at the decomposition of correlators $\langle \Delta\Delta^{\dagger} \rangle$ under Wick's theorem the contribution to the antiferromagnetism in the canonical ensemble with fixed projection of spin is suppressed (the values $\langle C_{\uparrow} C_{\downarrow}^{\dagger} \rangle$ are equal to zero), i.e., if the large-size off-diagonal order takes place, it will necessarily manifest itself on the background of the weak antiferromagnetism. In fact, we obviously see only the antiferromagnetic ordering, which indicates a complete absence of the superconducting correlations in the given temperature range.

[55] F. F. Assaad, W. Hanke, and D. J. Scalapino, Phys. Rev. B **50**, 12 835 (1994).